Earth Planet. Sci. Lett. 679 (2026) 119849

Contents lists available at ScienceDirect

Earth and Planetary Science Letters

journal homepage: www.elsevier.com/locate/epsl

Geochemical controls on the formation of lithium brines in closed-basins of the Lithium Triangle

Gordon D.Z. Williams [a], Julien Barre [b], Pascale Louvat [c], Sylvain Bérail [b], Romain Millot [d], Avner Vengosh [a,*]

[a] Division of Earth and Climate Science, Nicholas School of the Environment, Duke University, USA
[b] Advanced Isotopic Analysis, Pau, France
[c] Université de Pau et des Pays de l'Adour, E2S UPPA, CNRS, IPREM, UMR 5254, Pau, France
[d] Lithium de France, 31 rue de la Redoute, F-67500 Haguenau, France

ARTICLE INFO

Editor: Dr Tristan Horner

Keywords:
Critical minerals
Geochemical divides
Evaporation
Salt precipitation
Lithium and strontium isotopes
Lithium triangle

ABSTRACT

Sustainable lithium mining is critical to the renewable energy transition. Closed-basin brines are a major source of lithium yet the processes governing lithium enrichment remain poorly understood. In the Lithium Triangle (LT) of South America, hypersaline brines display anomalously high lithium concentrations including at the Salar de Uyuni (SDU) in Bolivia. Using new geochemical and isotopic data from the SDU, Bolivia, we update the accepted conceptual model of evaporative concentration and sequential mineral precipitation based on the formation of calcite, gypsum, and halite. Here we identify ulexite (Na-Ca-borate) precipitation as a previously overlooked but key process in the evaporative evolution of inflow waters that fundamentally alters brine chemistry prior to halite saturation. Additionally, we reveal that surficial brines are largely disconnected from the major lithium inflow, and instead their chemistries are controlled by cyclic halite dissolution-precipitation, leading to the conservative enrichment of solutes like lithium, boron, and magnesium. We suggest that deep brines exploited for lithium extraction are fossil and reflect different stages of evaporation, while modern processes make little contribution to the solute and lithium balance. This new conceptual model revises the classic geochemical pathway and has broad implications for lithium brines and resource sustainability across the LT.

1. Introduction

Lithium is an element critical to the global clean-energy transition primarily for use in Li-ion batteries and electric vehicles (IEA, 2021). Currently, ~40% of Li production is from Li-rich brines extracted from closed-basins in the Lithium Triangle (LT) of Chile, Argentina, and Bolivia (Fig. 1A) and the Tibetan Plateau in China (Jaskula, 2024; Moon, 2024).

Among the factors paramount to the generation of Li-rich brines is an arid climate with intense evaporative concentration of inflows to closed-basins (Munk et al., 2025). While the ultimate sources of Li to inflows varies (e.g. geothermal waters, rock weathering)(Álvarez-Amado et al., 2022; Cortes-Calderon et al., 2025; Godfrey and Álvarez-Amado, 2020; Meixner et al., 2022; Munk et al., 2025, 2018; Sarchi et al., 2023), it is well established that many brines of the LT developed along a similar sequence of evaporation and mineral precipitation (geochemical pathway)(Boschetti et al., 2007; López Steinmetz et al., 2018, 2020; Risacher et al., 2003; Risacher and Fritz, 1991a, 2009), including the sequential precipitation of calcite ($CaCO_3$), gypsum ($CaSO_4{\cdot}xH_2O$), and halite (NaCl) following intense evaporation. The final composition of brines are typically Na-Cl-(SO_4) (Risacher and Fritz, 2009) (classified following Eugster and Hardie, (1978)), occasionally with enrichments of Ca or Mg (Lowenstein and Risacher, 2009; Risacher et al., 2003; Risacher and Fritz, 2009). These processes also govern the enrichment of Mg, Li and B in the residual brines (Eugster and Jones, 1979; Risacher and Fritz, 2009). While the precipitation of calcite, gypsum, and halite are important steps in the evolution of closed-basin Li-rich brines, borate minerals like ulexite ($NaCaB_5O_9{\cdot}xH_2O$) are also prevalent throughout the LT (Fig. 1B). The precipitation of borates can control the boron isotope geochemistry of brines (Oi et al., 1989; Palmer and Helvaci, 1995) including those from the LT (Borda et al., 2023; Kasemann et al., 2004), however their role in controlling brine major ion chemistry has not been established.

Among these deposits is the Salar de Uyuni (SDU) in Bolivia, the

* Corresponding author.
E-mail address: vengosh@duke.edu (A. Vengosh).

https://doi.org/10.1016/j.epsl.2026.119849
Received 6 September 2025; Received in revised form 18 December 2025; Accepted 11 January 2026
Available online 21 January 2026

largest salt flat and Li-brine resource in the world (Gruber et al., 2011; Jaskula, 2024; Risacher and Fritz, 1991b; YLB, 2019). The SDU occupies the lowest basin of the Altiplano and formed through a series of large paleolakes that, either directly or through spillover, connected it to the other major, more northern and higher-elevation basins of the Altiplano, including the modern-day Lake Titicaca, Lake Poopó, and Salar de Coipasa (Fig. 1) (Baker et al., 2001; Fornari et al., 2001; Servant and Fontes, 1978). These oscillations between wet intervals with extensive paleolakes and arid intervals marked by lake desiccation are reflected in the SDU stratigraphy as alternating lacustrine sediments and halite/gypsum crusts (Baker et al., 2001; Fornari et al., 2001). Consequently, some of the salts in the SDU basin (brines and salt crust) were derived from spillover from these higher basins and from the recycling of earlier salt crusts (Grove et al., 2003; Risacher and Fritz, 2000, 1991b).

However, Placzek et al. (2011), using $^{87}Sr/^{86}Sr$ paleo-hydrologic mass-balance models, demonstrated that the last several lake cycles primarily received water and solute inputs from the southern Altiplano, suggesting that the solute sources feeding the Uyuni basin during these periods were broadly similar to those of today (i.e., inflow of the Rio Grande; Fig. 1). Likewise, $^{87}Sr/^{86}Sr$ measurements of authigenic sediments from an SDU core (to ~50 m depth) indicate that inputs during these most recent lake cycles were relatively consistent (Nunnery, 2012). This is especially relevant because, at the SDU, brines are pumped from sediment and halite layers formed during these paleolake stages, down to 50 m (Williams and Vengosh, 2025; YLB, 2019). The most recent of the large lake cycles occurred between ~24 and 15 ka and its desiccation would have formed the uppermost salt crust at the SDU (Baker et al., 2001; Fritz et al., 2004) with a more recent shallow saline lake connecting the SDU to the Coipasa and Poopó basins between ~13 and 11 ka (Nunnery et al., 2019; Placzek et al., 2006, 2013) and possible minor shallow lacustrine episodes continuing until ~6 ka (Nunnery et al., 2019).

Today, the SDU is hydrologically isolated from the higher basins with respect to surface flow and receives most of its water and solutes from the Rio Grande (RG) in the south (Fig. 1) (Risacher and Fritz, 1991b). As the waters of the RG evaporate along the transport in the Rio Grande delta, they evolve into a hypersaline, Li-rich brine following the same geochemical pathway common to brines of the LT (Rettig et al., 1980; Risacher and Fritz, 2000, 1991b). Deeper groundwater flow and inputs to the SDU have never been quantified or characterized and are beyond the scope of this work. However, in general leaking of brines through the bottom of closed-basins and redissolution of deep evaporites in the LT has been demonstrated to be a potential source of solutes to brackish and saline inflow waters found throughout the LT including in geothermal waters (Risacher et al., 2011, 2003; Risacher and Fritz, 2009). The generation of new solutes to this water cycle, however, are typically derived from interactions of volcanic rocks with low salinity waters (Risacher et al., 2011, 2003; Risacher and Fritz, 2009).

Here, we reevaluate the conceptual model for the evolution of inflows to closed-basins of the LT by comprehensively assessing the geochemical evolution of inflows and brines from the SDU. We use new geochemical and isotope analyses (δ^7Li, $^{87}Sr/^{86}Sr$, $\delta^{18}O$, δ^2H) in SDU brines and inflows, combined with published chemical and isotopic data in waters and brines from the SDU and other LT basins. The integrated data reveal that several additional geochemical mechanisms have major impacts on developing brine geochemistry. Furthermore, brines within the salt crust often vary in composition (Risacher and Fritz, 1991b) and we provide new constraints on understanding these processes and the link between fossil and modern brine formation. Since the SDU and

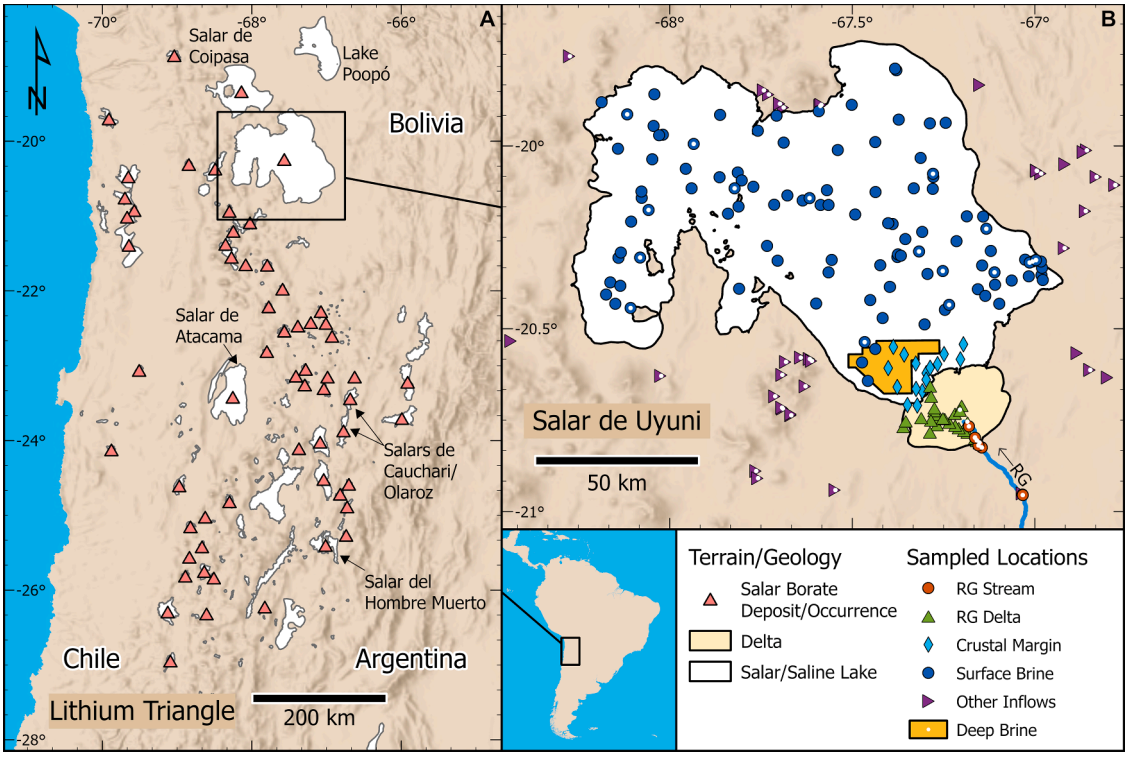

Fig. 1. Map of the Lithium Triangle and SDU. (A) The Lithium Triangle between Argentina, Chile and Bolivia hosts many closed-basin salar and saline lake brines (white spaces). Many of these closed-basins have recent borate (typically ulexite) deposits and occurrences (pink triangles) associated with brines and inflows. Several notable salars are also labeled. (B) Sampling map of the Salar de Uyuni, Bolivia with sample groups discussed in the text. This includes samples from the compiled dataset and those collected as part of this study that are deonted with a white dot including all deep brines. Surficial brines (blue circles) are from across the SDU. The deep brines were collected from wells (~16–50 m deep) in the shaded region, more specific locations are not available. Samples from along the Rio Grande's flow through the delta and into the salar are shown as well. The salt crust is shown in white. Data for borate deposits and occurrences from Alonso and Viramonte (1990) and; Orris (1995) and salar locations and shapefiles from Mihalasky et al. (2020) and ESRI (esri.com).

many closed-basins in the LT have similar geology and brine geochemistry (López Steinmetz et al., 2020, 2018; Risacher and Fritz, 2009), our findings are broadly applicable and aid in understanding the mechanisms controlling the brines' uniquely elevated Li concentrations and the sustainability of Li extraction from these salar systems.

2. Materials and methods

2.1. Sample collection and data compilation

Samples were collected over three sampling campaigns, in the dry season, May of 2023 and September of 2024, and the wet season, March of 2024. Surficial brines ($n = 19$) were collected from 0–30 cm below the salt crust surface across the SDU either from natural dissolution pits or from hand dug holes in the salt crust (all samples from the crustal margin are from the compiled dataset, section 2.2). Dissolution pits were common for samples from the east and non-existent to the west. Sample collection for deep brines and evaporation ponds are described in Williams et al. (2025a) and Williams and Vengosh (2025). Briefly, deep brines ($n = 8$) were collected from discharge pipes of pumped wells in the shaded region in Fig. 1B near the southeastern section of the SDU and represent an aggregate sample of several nearby wells, thus exact locations are not available. Each of these samples, however, is from a network of wells covering different sections of the deep brine pumping region in Fig. 1 meaning that these samples represent the entire shaded region. The screened depth is approximately 16–50 m b.g.l. These deep brines are discharged into a series of eight sequential evaporation ponds, and each pond was sampled from the central region. Inflow waters ($n = 75$) including those from the RG stream and RG delta were collected from streams throughout the SDU basin and nearby areas.

All water and brine samples were collected following the same methods (Williams et al., 2025b, 2024; Williams and Vengosh, 2025). Samples were filtered with 0.45 μm mixed cellulose ester filters fitted to a syringe. For cation, trace metal, Li isotope, and Sr isotope analyses samples were collected in acid-washed high-density polyethylene (HPDE) bottles and acidified with Fisher brand optima grade HNO_3. For anion and alkalinity analyses samples were collected in cleaned HDPE bottles without headspace. Unfiltered samples were collected without headspace in soda glass exetainers with butyl rubber septa for dissolved inorganic carbon (DIC) analyses and collected in borosilicate glass exetainers with silicone/PTFE septa for O and H isotope analyses.

2.2. Analytical procedures

Major and trace metals were measured at Duke University, USA. Ion chromatography (IC) was used to measure major cations (Li^+, Na^+, K^+, Mg^{2+}, and Ca^{2+}) with a Thermo Scientific Aquion IC and anions (Cl^-, Br^-, SO_4^{2-}) with a Dionex IC DX-2100. A Thermo Fisher Scientific X-series II quadrupole inductively coupled mass spectrometer (ICP-MS) was used to measure B. The accuracy of analyses was monitored by regular measurements of the IAPSO Atlantic seawater standard (Williams et al., 2025a).

Radiogenic Sr isotopes ($^{87}Sr/^{86}Sr$) were measured with a Thermo Fisher Scientific Triton thermal ionization mass spectrometer with single Re filaments at Duke. 1000–2000 ng of Sr were purified using Eichrom Sr-specific resin (Hall et al., 2025). The accuracy and reproducibility of analyses were monitored by repeated measurement of NIST SRM 987 at 0.710252±0.000010 ($n = 71$) and the IAPSO Atlantic seawater standard at 0.709166±0.000009 ($n = 10$), in good agreement with other published values (Jochum et al., 2005).

Li isotopes were measured at both Advanced Isotopic Analysis (AIA), France, and Duke using multi-collector ICP-MS (MC-ICP-MS). At AIA a Nu Plasma MC-ICP-MS was used and at Duke a Nu Sapphire MC-ICP-MS was used. Purification of Li in both labs used AG 50W-X12 (200–400 mesh) resin (Bio-Rad) with 100–1000 ng of Li and eluted with 0.2 M HNO_3. Samples were regularly monitored to ensure full recovery of Li from the columns and separation from Na. $^7Li/^6Li$ ratios were normalized to IRMM-016 following standard-sample bracketing during each run (Millot et al., 2004). Values are reported as δ^7Li where $\delta^7Li = ([^7Li/^6Li]_{sample}/[^7Li/^6Li]_{IRMM\text{-}016})\text{-}1)*1000$. A comparison of a natural brine sample between the two labs is shown in Fig. S10. The IAPSO Atlantic seawater standard was monitored for accuracy resulting in a value of 31.4±0.9‰ ($n = 12$), in good agreement with the accepted value of 31.0‰ to 31.2‰ for seawater (Jochum et al., 2005; Millot et al., 2004).

DIC concentrations and O and H isotopes were measured at the UC Davis stable isotope facility. DIC was measured by CO_2 evolution to headspace after treatment with phosphoric acid and analyzed on a Thermo Scientific GasBench II coupled to a Thermo Finnigan Delta Plus XL isotope-ratio mass spectrometer (IRMS). O and H isotopes in water were measured by headspace equilibrium with CO_2-He and H_2-He gas for O and H respectively. O in headspace CO_2 was measured on a Thermo Scientific GasBench II coupled to a Thermo Finnigan Delta Plus XL IRMS and H in headspace H_2 was measured on a Thermo Scientific GasBench II coupled to a Thermo Electron Delta V Plus IRMS. Replicate analysis of reference materials for O and H across the mass range yield a precision of ±0.04‰ for $\delta^{18}O$ and of ±1.1‰ for δ^2H referenced to VSMOW.

All new data measured for this study are in tables S1 through S4.

2.3. Data compilation

Data were compiled from several sources that have reported elemental and isotopic data in and around the SDU (Ericksen et al., 1978; Grove et al., 2003; Haferburg et al., 2017; Meixner et al., 2022; Placzek et al., 2011; Rettig et al., 1980; Risacher, 1992; Risacher and Fritz, 1991b; Schmidt, 2010; Sieland, 2014; Sieland et al., 2011; Williams and Vengosh, 2025, 2025) and from salars and inflows around the LT (Borda et al., 2023; Garcia et al., 2020; Godfrey et al., 2013; López Steinmetz et al., 2020, 2018; Moraga et al., 1974; Muller et al., 2020; Rettig et al., 1980; Risacher, 1992; Risacher et al., 1999; Risacher and Fritz, 1991a). Compiled data varied in terms of the completeness of data reported and the units (i.e. mg/L versus mg/kg). For the SDU most data was either reported on a per kg basis or had a reported density value so all datapoints were converted to mmol/kg while across the LT most samples were reported on a per L basis often without a density value and are shown as mmol/L. This makes no difference for the discussion and comparison of elemental ratios (Na/Cl and B/Li) across the LT. All compiled data used in this study are in tables S1 through S5. Data shown in boxplots for brines and inflows from throughout the LT are the mean value for each basin.

2.4. Modeled parameters

For all modeling PHREEQC (v 3.7.3) was used with a Pitzer ion interaction model (Parkhurst and Appelo, 2013). For all modeled results, only samples with complete chemistry were used, reporting, at a minimum, measurements and concentrations of pH, Li, Na, K, Mg, Ca, Cl, SO_4 and with an absolute charge balance of ≤5%. Saturation indices (SI), specific conductivity (SPC), and the contributions of borate alkalinity (BA) to total alkalinity (TA) were calculated with this model. SPC was modeled at 25°C; BA and TA were modeled for brines following the methods of Williams et al. (2025a) and is only shown for samples collected as part of this study since DIC was measured directly rather than by titration.

2.5. Statistical analyses

All statistical analyses were performed in MATLAB (v 9.13.0). Nonparametric analyses were performed including Spearman's rank correlation where rho (ρ) represents the correlation coefficient and the p-value (p) indicates significance. Linear correlations were performed as specified where r^2 represents the correlation coefficient and p indicates

significance.

3. Results and discussion

3.1. Deltaic evolution of inflows

Throughout the LT, dilute inflows to closed-basins commonly exhibit Na/Cl molar ratios >1 due to water-rock interactions with the local andesitic to dacitic volcanic terrain (Risacher et al., 2003; Risacher and Fritz, 2009). In contrast, associated hypersaline brines typically have Na/Cl ratios <1 (Risacher et al., 2003; Risacher and Fritz, 2009). Since halite is the major Na mineral and removes Na and Cl in equimolar proportions, evaporation of inflow waters with Na/Cl ratios >1 should yield brines with Na/Cl >>1 (Hardie and Eugster, 1970). This persistent mismatch suggests a common mechanism modifying Na/Cl ratios prior to halite precipitation. Furthermore, mineral precipitation sequences in brines of the LT are typically considered to terminate at the halite precipitation stage (Risacher and Fritz, 2009) yet evaporation ponds at Li and K saltworks demonstrate that additional salts can form following the halite stage (Garrett, 2004; Pueyo et al., 2017; Williams and Vengosh, 2025), implying similar natural processes may occur along evaporation paths.

To understand the evolution of the brines in the SDU, we investigate three defined sections along the Rio Grande flow; (1) the RG stream, (2) the RG delta composed of shallow groundwaters (<2 m deep) within the deltaic sediments, and (3) the crustal margin brines located in the salt crust along the southeastern edge of the SDU (Fig. 1B). Additionally, we investigate deep brines from ~16–50 m below the salt crust also from the southeast (Fig. 1B), which are the primarily source for Li extraction and their relationship to the RG is discussed in section 3.3.

The RG stream is brackish, ~2 g/kg TDS, and becomes hypersaline while flowing through the RG delta reaching a TDS of ~310 g/kg at the crustal margin. This is a process driven by evaporation (Rettig et al., 1980; Risacher and Fritz, 1991b), confirmed by a lower $\delta^{18}O$ vs $\delta^{2}H$ slope than the local meteoric water line (Fig. S1) and resulting in extremely elevated Li and B concentrations up to 530 mmol/kg Li and 314 mmol/kg B (Fig. S2). During evaporation, the three classic geochemical divides are observed (calcite, gypsum, halite) where the equimolar removal of ions to precipitating minerals enriches the predominant ion in the residual brine and depletes the other (Hardie and Eugster, 1970). Calcite precipitation enriches Ca and depletes DIC (Fig. 2A); gypsum precipitation enriches SO_4 and depletes Ca (Fig. 2B); and halite precipitation enriches Cl and depletes Na (Fig. 2C) in the most evolved brines. These geochemical processes result in a brine composition of SO_4>>Ca>DIC and Cl>>Na.

At the onset of halite precipitation, the Na/Cl ratio of the RG delta is ~0.8–0.9. However, the RG stream flowing into the delta is ~1 or slightly greater, indicating that Na is removed from groundwater within the delta. Na-sulfate salts do not form in the delta (Risacher and Fritz, 1991b). Therefore, in the absence of other Na-salts we propose that Na is removed by ulexite, a Na-Ca-borate, which forms throughout the delta (Risacher and Fritz, 1991b). This mechanism explains the decrease in Na/Cl prior to the halite precipitation stage. This is supported by the concurrent decline in B/Li and Na/Cl ratios in the RG delta prior to halite precipitation, reflecting the preferential removal of B and Na (Fig. 3A). This indicates that ulexite is an important step and an unrecognized geochemical divide, shifting the Na/Cl ratio from ~1 to <1, facilitating the development of a brine where Na/Cl<<1 following halite precipitation. Similarly, Ca/SO_4 is >1 in the RG stream, yet the brine evolves to Ca/SO_4<1, due to both calcite and ulexite precipitation, preferentially removing Ca from the evaporating brines.

At the salt crust, RG-derived brines feed into perennial pools that continue to evaporate (Risacher and Fritz, 1991b), driving further halite precipitation and eventually the saturation of additional salts. To better understand this evolution and the additional mineral precipitation sequences, we use data from artificial evaporation ponds at the SDU, operated for Li and K recovery (Williams et al., 2025a; Williams and Vengosh, 2025), an approach commonly employed to understand seawater (e.g. McCaffrey et al., 1987) and brine (e.g. Pueyo et al., 2017) evaporation trends. In these ponds minerals precipitate in the sequence of halite, sylvite (KCl), mixed K-salts, Li-sulfate ($Li_2SO_4{\cdot}xH_2O$), and bischofite ($MgCl_2{\cdot}xH_2O$) (Williams et al., 2025a; Williams and Vengosh,

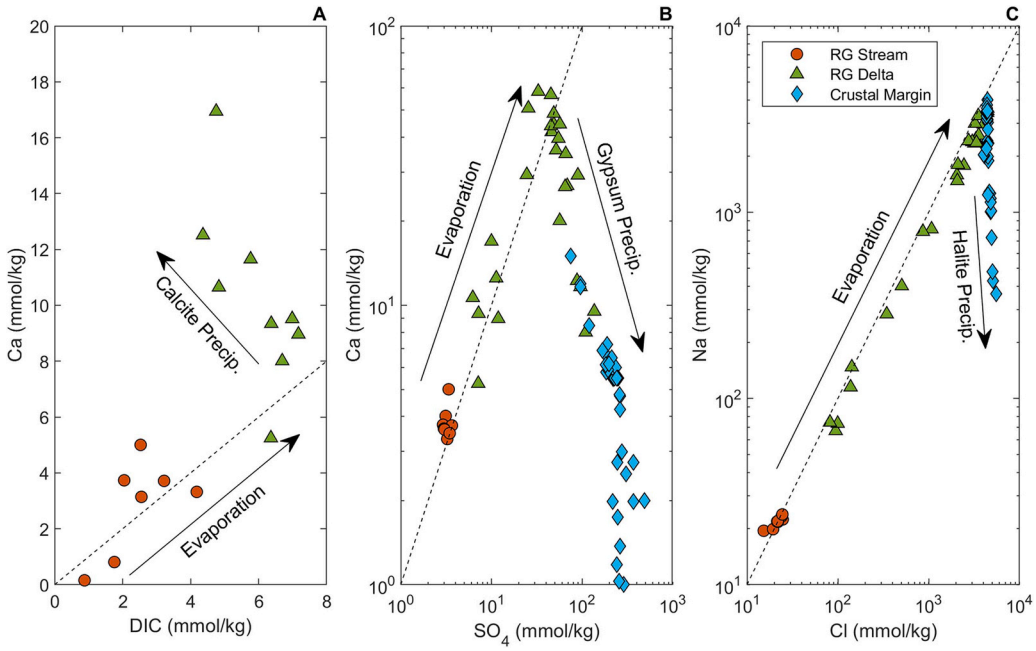

Fig. 2. The classic geochemical divides. Geochemical divides during the evaporative concentration of the Rio Grande and associated delta waters. Dashed lines are 1:1 lines. (A) The calcite divide: the initial Ca concentration is typically greater than that of DIC and during precipitation of calcite (equal removal of Ca and DIC), Ca becomes more concentrated in the residual brine. (B) The gypsum divide: gypsum removes equal parts Ca and SO_4. While Ca concentration is greater than that of SO_4 throughout the delta and inflow waters, SO_4 becomes more enriched relative to Ca in the residual brines. (C) The halite divide: Na and Cl are equally removed with halite precipitation and Cl becomes more concentrated in the residual evaporated brines.

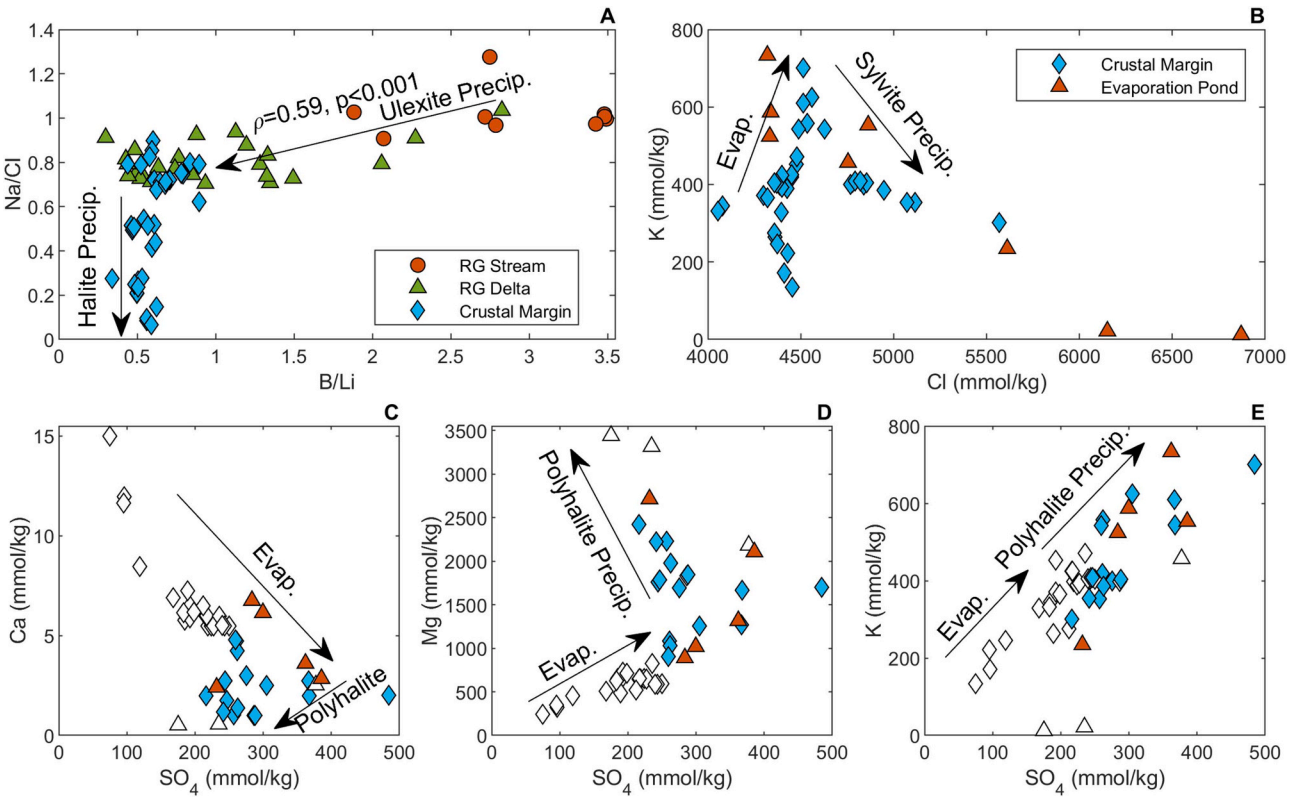

Fig. 3. Geochemical divides identified during the evolution of brines at the SDU. Three key new geochemical divides are identified: (A) Ulexite, (B) Sylvite, and (C–E) Polyhalite. (C–E) Open-face markers are brines undersaturated with respect to polyhalite, while closed-face markers are supersaturated brines. Super saturation of polyhalite appears to occur at the inflection point between SO_4 and both Ca and Mg, while K and SO_4 become coenriched in the residual brines. Data from evaporation ponds (red triangles) are shown for reference.

2025; YLB, 2019). While these evaporation pond brines evolve in sequential ponds where they no longer interact with previously precipitated salts (i.e. the final ponds will not be interacting with halite), a process somewhat distinct from the continuously evaporating natural ponds of the SDU, the chemistry of evolving crustal margin brines roughly mimic those of the artificial evaporation ponds.

In the natural crustal margin samples, following halite saturation, a sylvite divide is apparent, where K becomes depleted and Cl enriched in the residual brine (Fig. 3B). Inflections between SO_4 and other major ion concentrations in solution (Fig. 3C–D) suggest that a sulfate salt is precipitating. This is likely polyhalite ($K_2Ca_2Mg(SO_4)_4{\cdot}xH_2O$), a K-Mg-Ca-sulfate, since at the inflection point between Mg and Ca with SO_4, polyhalite reaches saturation (Fig. 3C–D). K and SO_4 however, appear to become co-enriched (Fig. 3E) reflecting the mixed K-salts reported in the evaporation ponds with sylvite and polyhalite precipitating concurrently. Regardless, the alignment of polyhalite saturation with the inflection ponds in the Ca vs. SO_4 and the Mg vs. SO_4 trends together verifies that this indeed reflects polyhalite precipitating. Previous studies have reported minor occurrences of sylvite (Rettig et al., 1980) and polyhalite (Risacher and Fritz, 2000, 1992) in the southeastern crustal margin of the SDU. During this stage, Li and B predominantly remain in solution and continue to concentrate (Williams et al., 2025a). Unlike the evaporation ponds, we find no evidence that natural RG-derived brines progress to the Li-sulfate precipitation stage (see supplemental text).

Overall, we demonstrate that RG-derived brines follow a series of geochemical divides in addition to those commonly accepted for the evaporative evolution of inflows to closed-basins of the LT (i.e., calcite, gypsum, and halite). Of these additional divides, ulexite precipitation is perhaps the most important, as it fundamentally alters brine chemistry prior to halite formation. Although the RG is the only major inflow to the SDU today and ulexite is actively forming there (Risacher and Fritz, 1991b), other inflows likely existed during past paleolake intervals. We therefore posit that ulexite precipitation was also an important process during these earlier periods. Supporting evidence includes: (1) the presence of ulexite deposits found elsewhere around the margins of both the SDU and the Salar de Coipasa, which were hydrologically connected, suggesting that evaporative concentration of paleo-rivers or streams produced borates through similar mechanisms (Orris, 1995; Risacher and Fritz, 1991b); and (2) limited sediment-core data from within the SDU exists, however there are some reported occurrences of borates within evaporite and lacustrine units beneath the modern salt crust (CAMIBOL, 2016), indicating that borate precipitation (presumably ulexite) took place during desiccation of former paleolakes.

3.2. *Geochemical mechanisms in surficial brines*

While brines evolved from the RG reach a high degree of evaporation at the southeastern crustal margin with TDS and Li up to 312 g/kg and 530 mmol/kg (3690 mg/kg) respectively (Risacher and Fritz, 1991b), the surficial brines across the SDU show lower salinity (TDS ~240–300 g/kg) and Li (~8–235 mmol/kg, ~55–1630 mg/kg; Fig. S3), rarely progress beyond halite precipitation (Fornari et al., 2001; Risacher and Fritz, 1991b), and follow distinctly different geochemical patterns. Inverse relationships between Na/Cl with Li, $\delta^{18}O$, and Br/Cl (Figs. 4, S4), indicate that solute concentrations of the surficial brines are controlled by recycling of the salt crust driven by halite dissolution from meteoric waters (e.g., Na/Cl~1, low Br/Cl, Li and $\delta^{18}O$) and subsequent evaporative precipitation (e.g., low Na/Cl, high Br/Cl, Li and $\delta^{18}O$).

Nearly all surficial brines at the SDU are saturated and appear to be in equilibrium with halite (Fig. S5). Halite is by far the most dominant mineral in the salt crust (~90–100%)(Fornari et al., 2001; Risacher and

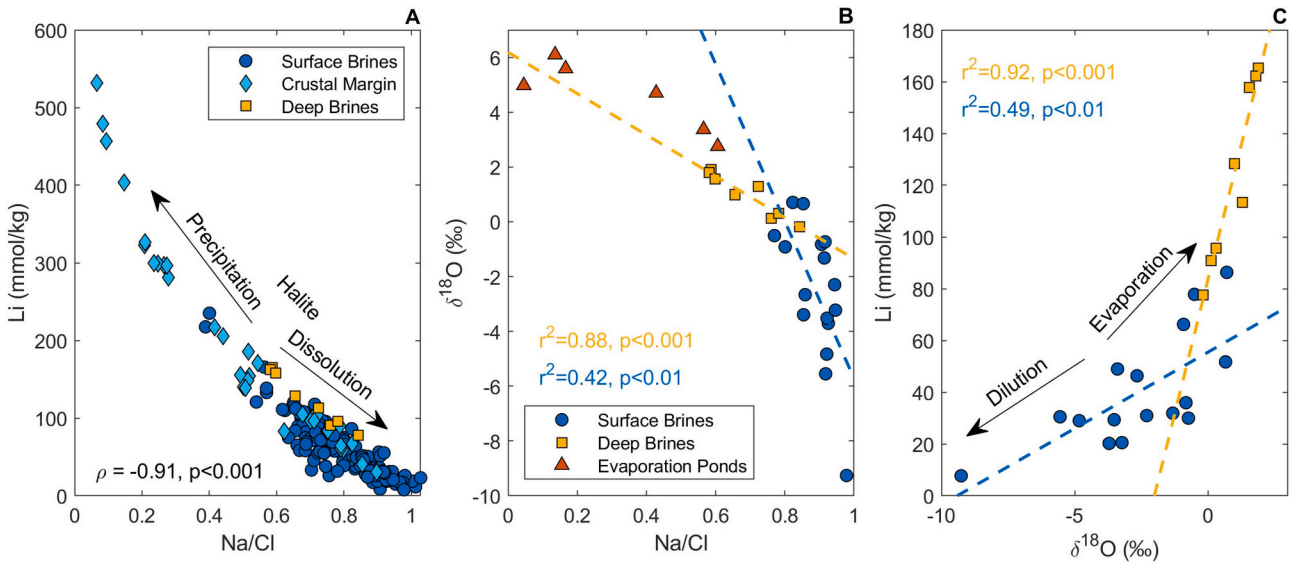

Fig. 4. (A) Lithium concentration variations versus Na/Cl reflects the halite continuum where evaporation and halite precipitation increases Li concentration and decreases Na/Cl, while halite dissolution decreases Li concentration and drives Na/Cl towards unity. (B) Variations and linear correlations between $\delta^{18}O$ and Na/Cl of the surficial brines, deep brines, and brines from evaporation ponds indicates that Na/Cl is decreasing as a function of halite precipitation during evaporation (higher $\delta^{18}O$). The lower slope of Na/Cl vs $\delta^{18}O$ of the deep brines align with that of the evaporation ponds, reflecting evaporation without the depleted (lower $\delta^{18}O$) meteoric water inputs seen in surficial brines. (C) Variations and linear correlations between Li concentrations and $\delta^{18}O$ showing that greater Li concentrations correspond to high $\delta^{18}O$ values due to evaporation. The lower Li and $\delta^{18}O$ values of surface brines reflect greater dilution by meteoric water. The relatively low correlation coefficient in the surface brines in B and C likely reflects isotopic variations across the large area of the SDU and its watershed.

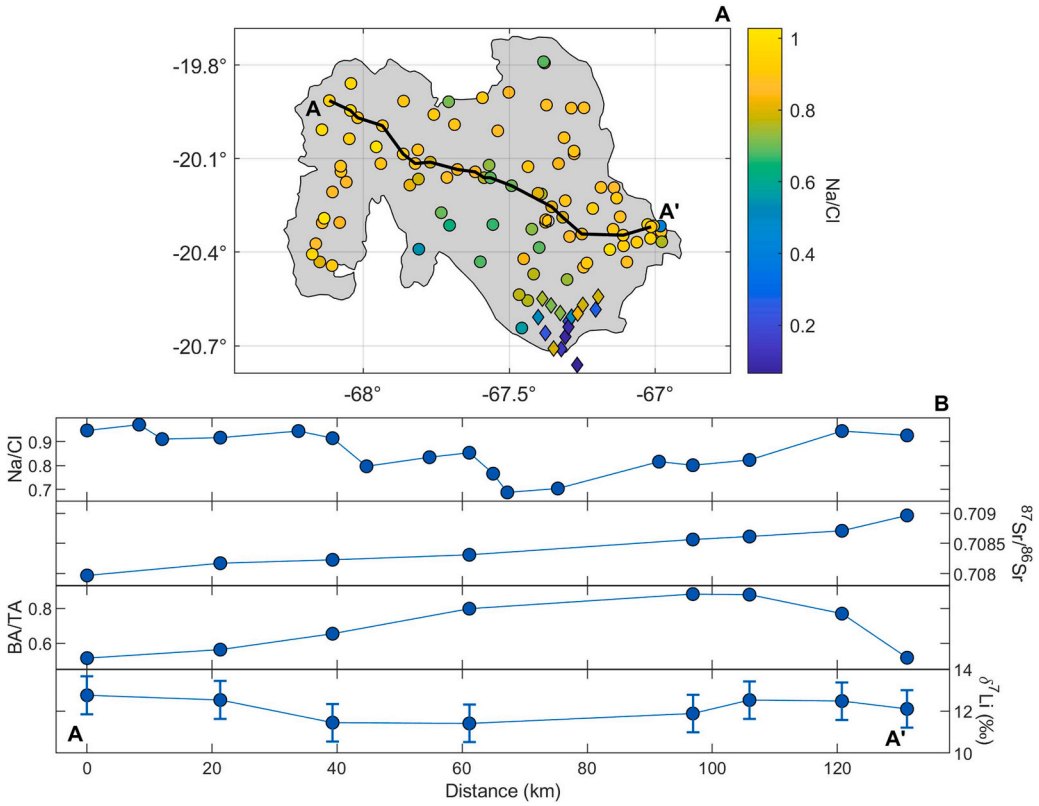

Fig. 5. Geochemical controls on solute concentrations in surficial brines. (A) Spatial variability of Na/Cl ratios (color range) in surficial brines from the SDU where the lowest values are brines located near the southeast crustal margin (diamonds), reflecting the greatest evaporative signature. Transect A roughly follows a west to east path. (B) Na/Cl, $^{87}Sr/^{86}Sr$, BA/TA (borate alkalinity to total alkalinity ratio), and $\delta^{7}Li$ in brines along transect A. The central portion of the SDU shows a more evaporated signature with lower Na/Cl and higher BA/TA than the eastern and western edges, which receive greater inputs from dilute inflows that dissolve halite and introduce higher DIC. The linearity of $^{87}Sr/^{86}Sr$ with distance (west to east) suggests mixing between eastern and western inflows characterized by more radiogenic $^{87}Sr/^{86}Sr$ ratios to the east and less radiogenic ratios to the west. The $\delta^{7}Li$ values along transect A are all within the analytical error of individual points and do not appreciably vary along the surfical brines of the SDU.

Fritz, 1991b) and accounts for the majority of solutes in the brine (average ~73 wt.% if all dissolved salts are precipitated). Additionally, annual flooding temporarily dilutes the surficial brines, partially dissolving the halite crust (Risacher and Fritz, 1991b), whereas evaporation during the dry season induces halite precipitation. This cyclic halite dissolution-precipitation controls the Li concentration in the surficial brines as evaporation removes water leading to halite precipitation and to lower Na/Cl and higher, $\delta^{18}O$, Br/Cl and Li concentrations (Fig. 4, S4), while dissolution does the opposite (i.e. halite dissolution increases the salt mass and volume of the brine thereby decreasing the Li concentration and vice versa during precipitation). The surface brine rarely exceeds halite saturation (Fig. S5), suggesting that a buffering mechanism prevents further evaporation. A similar pattern was observed at the Salar de Atacama in Chile, where evaporation is dampened as the brine drops below the salt surface and reaches an evaporation extinction depth (Marazuela et al., 2019). Since the surficial brine of the SDU drops below the salt crust during the dry season, this should limit the evaporative process and therefore caps the degree of Li enrichment in the surficial brines. This mechanism is distinct from the evaporative process at the RG delta, along the crustal margin, where the brine feeds into perennial surface pools that can continuously evaporate and reach much higher Li concentrations (Fig. 4A)(Risacher and Fritz, 1991b), resulting in the mismatch in Li concentrations compared to surficial brines. A similar trend is observed for Ca/SO_4 ratios since gypsum is the second most prevalent mineral in the salt crust (<10%, Fig. S6)(Risacher and Fritz, 1991b).

Na/Cl ratios, Li concentrations, and $\delta^{18}O$ can record signatures of more evaporation or dissolution brine regimes. Fig. 4 shows that $\delta^{18}O$ increases with increasing Li concentration and with decreasing Na/Cl, demonstrating that evaporation controls halite precipitation and therefore Li concentration. Furthermore, variations in Na/Cl ratios across the SDU demonstrate the greater evaporative signatures are present closer to the center of the salt crust. This can be seen in an east-west transect (Fig. 5), where the Na/Cl ratios are lower, ~0.70, in the center of the salt crust and higher, ~0.95, closer to the edges. The high values closer to the edges of the salt crust reflect a greater influx of dilute inflows (surface runoff and groundwater upwelling/discharge, see supplemental text) and the consequential halite dissolution while the central portion of the salar receives less direct runoff and maintains a more evaporated signature with lower Na/Cl.

Radiogenic Sr isotopes ($^{87}Sr/^{86}Sr$) can detect solute sources to the surficial brines. Previous studies have shown that waters from the eastern and western mountain ranges have distinct $^{87}Sr/^{86}Sr$ values with a more radiogenic signature, ~0.7110, to the east and a far lower ratio, ~0.7069, to the west (Grove et al., 2003; Placzek et al., 2011), reflecting the distinct geology of the eastern and western mountain ranges. Our data of streams to the east and west of the SDU are consistent with this distinction (Fig. 6A, S7). Consistently, the $^{87}Sr/^{86}Sr$ of the RG, which is the largest modern solute source to the SDU in the southeast is 0.7095, after mixing from both eastern and western tributaries (Grove et al., 2003). Despite the large range in $^{87}Sr/^{86}Sr$ of inflows, the surficial brines maintain a relatively homogenous $^{87}Sr/^{86}Sr$ signature, between 0.7080 and 0.7091 (Fig. 6A). Within this narrow range, the $^{87}Sr/^{86}Sr$ values along the west-east transect show a linear correlation with distance (Fig. 5B, r^2=0.96, p<0.001), suggesting a mixing gradient between eastern and western brines influenced by local inflows and likely driven by the annual flooding. While mixing is clearly happening, this process yields no significant (p>0.05) correlations between major-ion concentrations and $^{87}Sr/^{86}Sr$, which are not fractionated during halite dissolution-precipitation, the major mechanism controlling solute concentrations in the surficial brines.

While Sr is a trace element in SDU brines (0.003–0.35 mmol/kg), $^{87}Sr/^{86}Sr$ is a conservative tracer, unaffected by dissolution and precipitation processes, thus we can use it to estimate the approximate fraction of Sr from external inflows to individual SDU brine samples. Placzek et al. (2011) estimated the $^{87}Sr/^{86}Sr$ of the last minor paleolake (~13–11 ka) covering the SDU was 0.70854 as recorded in carbonates. We assume that this value is the initial $^{87}Sr/^{86}Sr$ value of the SDU surface brines prior to influences from modern inflows (i.e. since the last paleolake). The average $^{87}Sr/^{86}Sr$ value of inflows from the west are 0.7069 and from the east are 0.7110 (Placzek et al., 2011). Assuming values greater than the initial brine value are only influenced by Sr inputs from the east and those lower than the initial are only affected by inputs from the west, we calculate the fraction of Sr from eastern and western inputs

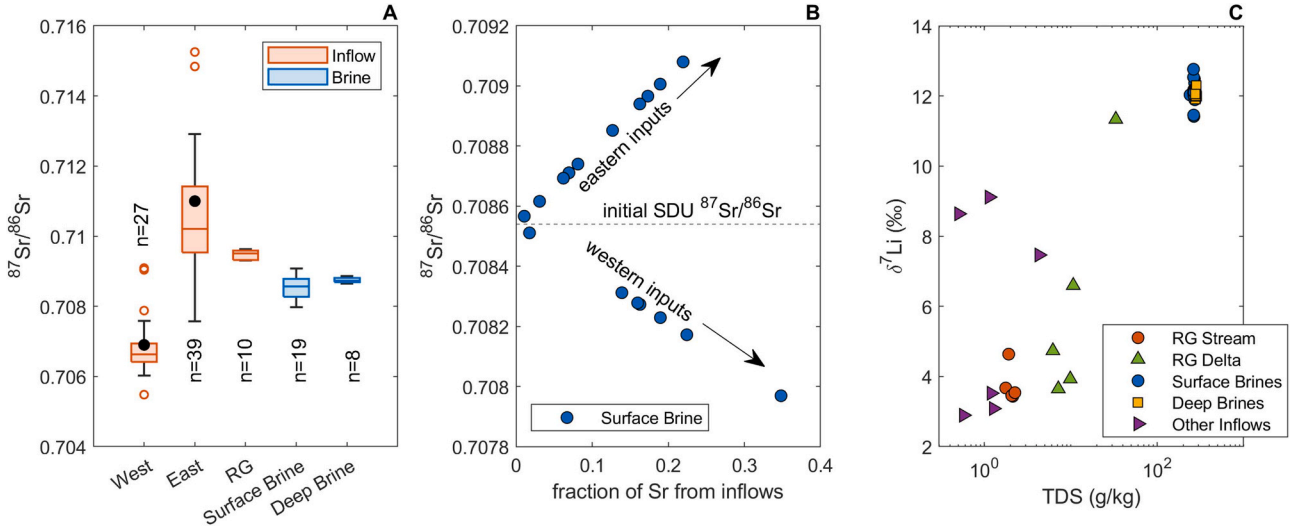

Fig. 6. (A) Box plots of the Sr isotope ratios of inflows and brines from the SDU. Inflow waters are divided by radiogenic $^{87}Sr/^{86}Sr$ ratios to the east and less radiogenic isotope ratios to the west, while the RG receives mixed inputs form the east and west and includes samples from the RG stream and RG delta. Deep and surface brines are relatively homogenous and indistinguishable. The range in values in the surficial brines reflects the variations of the inflows from the east and west. Black dots on the eastern and western inflow boxplots reflect the average Sr isotope values reported in Placzek et al. (2011). (B) Assuming an initial Sr isotope ratio of 0.70854 for the SDU brines reported by Placzek et al. (2011), the variations of the $^{87}Sr/^{86}Sr$ ratios in the surface brines are used to quantify mixing proportions between the initial brine and western and eastern inflows. (C) δ^7Li versus TDS in samples collected in this study. We observed an increase in δ^7Li from the RG stream (~4‰) through the delta (~11‰), reflecting isotope fractionation associated with Li interaction with deltaic sediments while evaporation increases TDS. Other inflows vary and may fractionate more or less along their flow to the SDU.

in each surface brine sample. Fig. 6B shows these results where the fraction of Sr input in individual surface brine samples from modern inflows varies from ~1% up to 35%. The greatest fractions are found in the eastern and westernmost brine samples from along the transect in Fig. 5A, at 35% and 22% respectively of modern Sr inputs while samples from throughout the SDU typically have much lower Sr inputs (Fig. 6B).

Dilute inflows also influence the alkalinity of the brines. Williams et al. (2025a) demonstrated that boron species control the alkalinity of brines at the SDU. We define borate alkalinity (BA) as the sum of alkalinity contributed by any boron species and assume that total alkalinity (TA) of the brines is dominated by species of boron and DIC. The contribution of BA to TA, BA/TA, increases from ~0.5 at the edges to ~0.8–0.9 toward the center of the SDU (Fig. 5B). We posit this reflects inputs of DIC from dilute inflows that have not undergone extensive evaporative concentration in a delta to remove DIC to calcite, thus inducing relatively low BA/TA near the salar margins.

Despite these clear influences from inflow waters, the δ^7Li values of surface brines are essentially homogenous at ~12‰ without any clear geographic variation (Figs. 5B, 6C). Li does not appreciably incorporate into halite (McCaffrey et al., 1987; Zherebtsova and Volkova, 1966), meaning that Li isotope fractionation should be minimal during halite dissolution-precipitation (Godfrey et al., 2013). By contrast, δ^7Li values in nearly all the freshwater inflows in the vicinity of the SDU are <8‰ (Fig. 5C). During water-rock interactions, ^{6}Li is preferentially incorporated into oxides and clay minerals, increasing δ^7Li in the residual water/brine (Penniston-Dorland et al., 2017). Such increases in δ^7Li have been observed in other salars in the LT (Álvarez-Amado et al., 2022; Garcia et al., 2020; Godfrey et al., 2013; Munk et al., 2018; Orberger et al., 2015), presumably caused by Li uptake to the clays and oxides of deltaic environments. Inflows from the RG show the same trend increasing from ~3 to 5‰ in the RG stream to ~11‰ in saline waters in the delta (Fig. 6C). Inflow waters (ground and surface inflows) from around the SDU are likely to also be interacting with clays or oxides thereby inducing Li isotope fractionation. The degree of fractionation would vary based on the magnitude of interaction with clays or oxides, meaning that not all inflows would reach to the same value of 12‰. However, our data show a homogeneous δ^7Li value with no spatial variation in the surficial brines along the edges of the SDU; essentially all samples along the east-west transect are the same value, within analytical error (Fig. 5B). Consequently, this would suggest that the dilute inflows do not significantly contribute to the overall Li budget of the SDU surficial brines. This is in contrast to the Sr inputs from modern inflows and may be explained by the fact that Li is a major element in the brines while Sr is a trace element and therefore more susceptible to isotopic shifts from dilute inflows with relatively low Li and Sr concentrations. We posit that the original source of Li in the surficial brines must have evolved through the same geochemical pathway, like we observed in the RG delta with a detectable Li isotope fractionation. We therefore suggest that the homogenous δ^7Li values of the surficial brines and similarity to the composition of the deep brines (see section 3.3) indicate that they originated from the desiccation of a well-mixed paleolake resulting in an isotopically homogeneous brine. While the RG inflow currently provides the major solute and Li input to the SDU today, our data suggest that other modern surficial or subsurface inflows likely do not provide significant inputs of major ions like Li, rather the major solutes and Li in SDU surficial brines are fossil reflecting the continuous recycling of brines and salts in the halite crust.

Overall, the geochemical, ^{87}Sr/^{86}Sr, and δ^7Li variations of the surface brines suggest that they are derived from a homogenous brine source with continuous modifications along the halite precipitation-dissolution cycles combined with minor inputs from modern inflows. Given these observations, we suggest that the surface brines originated from relict brines preserved from the desiccation of a well-mixed paleolake. The desiccation of a paleolake has previously been posited as the source of brines and the salt crust in the SDU (Risacher and Fritz, 1991b). However, the solutes concentrations such as Li in the surface brines across the SDU are controlled by modern processes of cyclic salt dissolution by meteoric water flooding and subsequent evaporation and halite precipitation. This explains the large variations in Li concentrations and the constant δ^7Li observed in the SDU surface brines. While paleolakes at the SDU likely recycled previous salt crusts and brines (Risacher and Fritz, 1991b), the last minor paleolake existed between ~13-11 ka (Placzek et al., 2013, 2011) meaning that the majority of solutes in the SDU brines are at least this old if not much older.

3.3. Deep brines

SDU deep brines from the southeast (Fig. 1B) were collected from production wells pumping from deeper halite crusts at ~16–50 m deep, extracted from mixed halite-sediments of paleo-salars (Baker et al., 2001; Williams and Vengosh, 2025). These brines have very similar chemistry to the surface brines with similar and yet not identical variations in Na/Cl, Br/Cl, and δ^{18}O and with slightly greater Li concentrations at the same Na/Cl ratios (Fig. 4A). Comparing Na/Cl vs δ^{18}O of the surface and deep brines, the deep brines fall on a lower slope (Fig. 4B). Extrapolating this trend to a Na/Cl ratio of 1 (i.e., pure halite dissolution) to estimate the original δ^{18}O value prior to evaporation and precipitation of halite, the deep brines extrapolate to a higher δ^{18}O value of -1.4‰ relative to the surficial brines, which extrapolate to -5.7‰ at a Na/Cl ratio of 1. The lower δ^{18}O value and steeper slope for the surficial brine reflects the direct connection to isotopically lighter meteoric waters driving the surficial halite dissolution. Stable isotope data from the artificial evaporation ponds, which are fed by the deep brines and which have little to no input from meteoric waters, infers that variations in their δ^{18}O are primarily driven by evaporation. The data for brines in the artificial evaporation ponds fall along nearly the same trend as the deep brines (Fig. 4B), suggesting that the slope of the deep brines reflects evaporation without the influence of regular meteoric water inputs driving halite dissolution as in in the surficial brines. This in turn suggests that deep brines are not influenced by modern processes. Furthermore, the linear correlations between Na/Cl with δ^{18}O and Br/Cl (Fig. 4, S4) might reflect different degrees of brine evaporation, similar to the patterns observed in the evaporation ponds, rather than the halite dissolution-precipitation trend seen in surficial brines. This might suggest that the apparent fossil deep brines in the southeastern section of the SDU are disconnected from modern meteoric water inputs distinct from the seasonal flooding of the surficial brines, resulting in higher δ^{18}O and Li concentrations.

The ^{87}Sr/^{86}Sr and δ^7Li values of the deep brines are indistinguishable from the surficial brines indicating that the solutes have a common origin and likely originated from the same source (Fig. 5). Additionally, the ^{87}Sr/^{86}Sr values of the deep brines (0.7087–0.7089) are identical to that of authigenic carbonates (0.7085–0.7089) formed from the last several paleolake cycles (since ~95 ka) as determined by Placzek et al. (2011) from carbonate samples collected throughout the SDU, Coipasa, and Poopó basins. It is important to note that the ^{87}Sr/^{86}Sr of the deep brines are somewhat different from that of the RG (0.7095; Fig. 6A) in spite of their close proximity (Fig. 1), further indicating their disconnect from nearby modern hydrologic processes.

Similar to the surface brines, we posit that the deep brines also formed from the desiccation of a relatively well-mixed and homogenous paleolake(s) that likely also recycled earlier salts and brines. While the surface brines are impacted by modern inflows that result in chemical variations along the halite-dissolution and precipitation cycle, the deep brines were likely originated from brines at different stages of evaporation, and consequently, have a higher Li content. Since these deep brines are formed from the desiccation of paleolakes and pumped from deeper salt crusts than the surface brine, it would stand to reason that these formed prior to the modern surface brine meaning that these deep brines are also fossil. While the region that these deep brines were pumped from is relatively small (~250 sq. km)(Williams and Vengosh, 2025) in comparison to the larger SDU (~10,000 sq. km)(Risacher and

Fritz, 1991b) (Fig. 1B), the findings presented here might suggest that the geochemical trends we see in the deep brines and are consistent for the surface brines across the entire SDU, might also be consistent in the deeper brine layers across the SDU. This however cannot be further verified with the available data.

For these reasons we posit that the deep brines, which are the brine source for Li extraction, are fossil brines trapped in deeper halite crusts at different stages of their evaporative evolution, where variations in Li concentration reflect different stages of fossil brine evaporation. This is somewhat distinct from the halite dissolution-precipitation mechanism seen in surficial brines that are affected by modern flooding with meteoric water across the SDU basin. Additionally, this could reflect the paleo-evaporative concentration of the RG since we see a similar process happening in the modern southeastern crustal margin near the RG delta. Consequently, the solute concentrations in fossil deep brines, are controlled by different geochemical processes than the surficial brines, explaining their higher Li concentrations.

3.4. Implications for brines throughout the lithium triangle

Integrating data from the SDU and other LT salars reveals how Li-rich brine chemistry evolves. The RG begins as a Na-(Ca)-(Mg)-Cl-(HCO_3)-(SO_4) brackish inflow and transitions to a Na-(Mg)-Cl-(SO_4) brine through evaporation and sequential mineral precipitation in the RG delta. Further evaporation and halite precipitation nearly depletes Na, producing a Mg-(K)-(Li)-Cl-(SO_4) brine (Fig. S8). This process follows the classic geochemical divide sequence (Eugster and Hardie, 1978; Hardie and Eugster, 1970), yet additional divides, notably ulexite formation, also influence brine chemistry by removing Na and enabling the formation of a Mg-dominant system in the residual Li-rich brines. Sylvite and polyhalite precipitation allow Li to further concentrate in the residual brines.

While the RG may be a major solute source to the SDU during wet periods (Baker et al., 2001; Grove et al., 2003; Risacher and Fritz, 2000, 1991b), our data indicate that it is largely disconnected from modern surficial brines away from the RG delta. Variations in chemistry are instead driven by (1) halite precipitation and dissolution controlling solute concentrations like Li, (2) mixing of eastern and western brines driven by dilute inflows inducing halite dissolution and modifying minor solute concentrations like Sr, and (3) contributions from residual fossil brines originated from the desiccation of a well-mixed paleolake.

Since halite cycling dominates brine chemistry and solutes vary along a trend with changes in Na and Cl (Fig. 4A), specific conductivity (SPC) should also vary along similar trends. Counterintuitively, SPC decreases with evaporation due to Na and Cl loss and increasing Mg dominance, meaning Li concentration rises as SPC falls, fitting a linear trend (r^2=0.88, $p<0.001$; Fig. 7A, S9). Consequently, in-field SPC measurements, paired with a calibrated regression, can quickly estimate Li concentrations offering a practical exploration tool due to the simplicity and low cost of conductivity meters.

The mechanisms controlling brine geochemistry observed at the SDU likely apply to closed-basins across the LT. Surveys show most closed-basin brines of the LT follow the same classic geochemical path, typically resulting in Na-Cl-(SO_4) brines (López Steinmetz et al., 2020, 2018; Risacher et al., 1999; Risacher and Fritz, 1991a, 1991b) with Na/Cl <1, despite inflows with Na/Cl >1 from the alteration of volcanic rocks (Fig. 7B). We propose that the precipitation of ulexite or other Na-borates, common to many salars (Alonso, 1999; Alonso and Viramonte, 1990; Chong et al., 2000; Ericksen and Salas, 1987) (Fig. 1A), remove Na and Ca from inflows and thus triggering a geochemical divide that results in brines with Na/Cl<1. Supporting this, B/Li ratios decline from inflows to brines, reflecting B removal to borate minerals (Fig. 7C). While Na-sulfate salts are found in some salars (Alonso and Viramonte, 1990; Vila, 1990), where borates may be less common, their role in reducing Na/Cl ratios during evaporation merits further investigation. Additionally, many brines of the Tibetan Plateau which is home to numerous closed-basin Li-rich brines, many of which have similar Na-Cl-(SO_4) chemistries and associated borate deposits (Garrett, 2004;

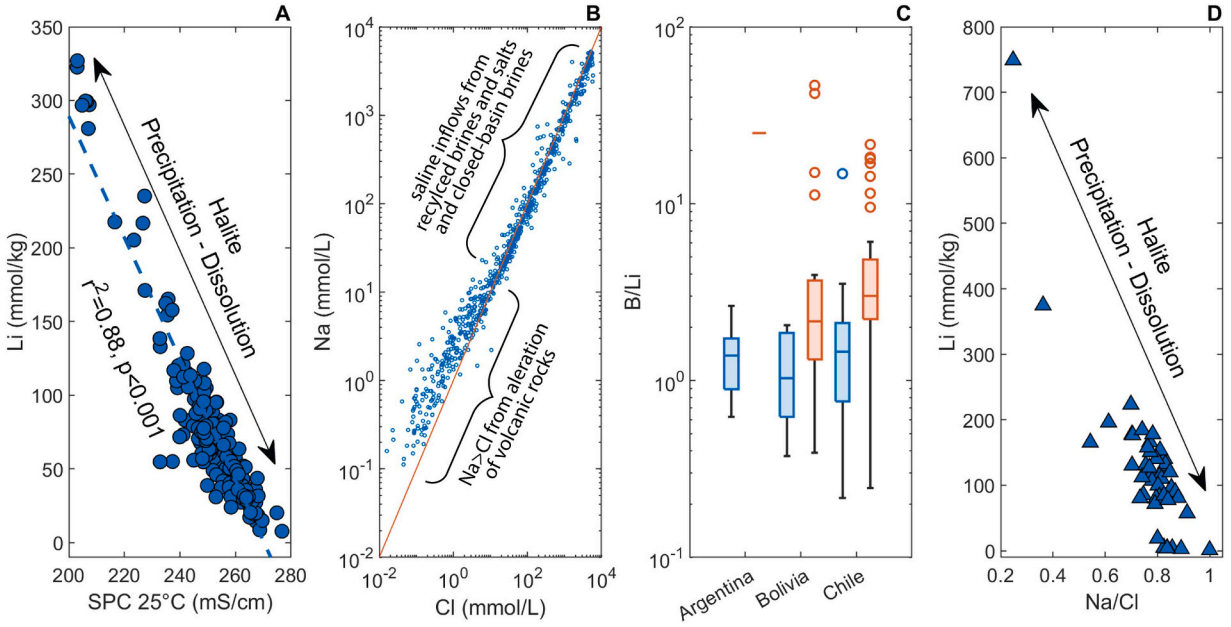

Fig. 7. Implications for other LT closed-basin brines. (A) lithium versus specific conductivity (SPC) of surficial brines from the SDU. The inverse linear correlations indicate that both Li concentration and SPC are controlled by halite precipitation and dissolution. (B) Na vs Cl plot modified from Risacher and Fritz (2009) shows that the generation of solutes in inflows from the alteration of volcanic rocks results in Na/Cl ratios >1 while saline inflows are derived from the recycled brines or the dissolution of salts; closed-basin brines are the evaporated products of these two inflow types resulting in Na/Cl ratios of ~1 or lower. The solid line is a 1:1 line. (C) Box plots of B/Li ratios in inflows and brines from different closed-basins of the LT. The Na/Cl and B/Li ratios of inflows to closed-basins of the LT are typically greater than those of the brines, reflecting preferential loss of Na and B, presumably to ulexite, and eventually Na to halite. (D) Lithium concentrations versus Na/Cl of brines (TDS>200 g/kg) from the Salar de Atacama. Data from Moraga et al. (1974). Data indicate that Li concentrations in brines are controlled by halite dissolution and precipitation falling along a clear trend much like at the SDU.

Zheng and Liu, 2009) suggesting that the findings here may be applicable beyond the LT as well, however an evaluation of this is beyond the scope of this paper.

Although most LT brines do not exceed halite saturation, persistent surface pools can continue evaporating, potentially forming sylvite or polyhalite. Indeed, these minerals have been observed at various salars (Bobst et al., 2001; Ericksen and Salas, 1987; Vila, 1990), suggesting they either formed from modern brines or during drier paleoclimates. Regardless, their presence underscores key events in modern or fossil Li-rich brine development across the LT.

Since Na and Cl are the primary ions in brines of the LT and halite and gypsum are the primary evaporite minerals in salar crusts (Ericksen and Salas, 1987), the same variations in surface brine chemistry associated with halite dissolution-precipitation are likely be present elsewhere in the LT, as demonstrated in Fig. 7D for the Salar de Atacama.

Overall, we integrate new and published data to reconstruct the evolution of dilute inflows to hypersaline brines at the SDU. We show that the evaporative evolution of modern inflows deviates from the classic sequence of mineral precipitation and are relatively disconnected from the surficial brines, which are controlled by modern meteoric water flooding and halite dissolution-precipitation cycling. By comparison, the deep brines pumped for Li production reflect fossil brines at different stages of evaporation, resulting in higher Li concentrations. In contrast, modern brine formation is limited geographically to the RG delta region and has little impact on the overall surficial and deep brines across the SDU. This infers that the brines used for Li production are fossil and are not replenished with Li or other solutes by modern processes and are at least as old as the most recent paleolake (i.e. >11 ka). This is consistent with observations at other brines throughout the LT that are considered fossil and are not replenished on modern timescales (ranging from tens to millions of years) (Munk et al., 2018; Risacher and Fritz, 2009) raising the question of the long-term sustainability of Li production in salar environments.

4. Conclusion

This study presents new geochemical and isotope data (Li, Sr, O, H) from inflows and brines of the SDU in Bolivia, integrated with a compiled geochemical dataset of waters and lithium-rich brines from other closed-basins across the LT, the region home to the majority of global Li resources (Jaskula, 2024). In addition to the classical geochemical pathway proposed for closed-basin brine evolution in the LT, our results demonstrate that borate mineral (ulexite) formation represents a critical early step that fundamentally alters the chemistry of the residual brines. The data show that both deep and surface brines in the SDU are fossil, derived from residual brines produced during the desiccation of paleolakes, whereas modern inflows from the surrounding basin contribute little to no lithium. Surface brines are, however, modified by meteoric flooding, which drives cyclic halite dissolution–precipitation processes that influence Li concentrations but not Li isotopic composition. In contrast, the deep brines likely formed through ancient evaporative concentration, leading to elevated lithium concentrations in the southeastern SDU. These findings refine our understanding of lithium enrichment mechanisms and highlight the limited natural replenishment of Li to closed-basin brines like the SDU.

CRediT authorship contribution statement

Gordon D.Z. Williams: Writing – review & editing, Writing – original draft, Visualization, Software, Methodology, Investigation, Formal analysis, Data curation, Conceptualization. **Julien Barre:** Writing – review & editing, Writing – original draft, Resources. **Pascale Louvat:** Writing – review & editing, Writing – original draft, Methodology. **Sylvain Bérail:** Writing – review & editing, Writing – original draft, Resources, Methodology. **Romain Millot:** Writing – review & editing, Writing – original draft, Methodology. **Avner Vengosh:** Writing – review & editing, Writing – original draft, Validation, Supervision, Resources, Project administration, Methodology, Investigation, Funding acquisition, Conceptualization.

Declaration of competing interest

The authors declare that they have no known competing financial interests or personal relationships that could have appeared to influence the work reported in this paper. Lithium de France had no role on data evaluation and interpretation in this study.

Acknowledgments

The authors would like the thank the Bolivian Ministry of Hydrocarbons and Energy and Yacimientos de Litio Bolivianos (YLB) as well as the Federación Regional Única de Trabajadores Campesinos del Altiplano Sur (FRUTCAS) for authorizing, facilitating, and accompanying the sampling missions at and around the SDU. We thank K. Ledebur (Andean Information Network) who provided invaluable logistical and field support and Y. Cruz (FRUTCAS) and R. Calizaya who provided substantial insight and support during the sampling campaigns. This study was supported by the Duke University Climate Research Innovation Seed Program, CRISP and the Duke University Josiah Charles Trent Memorial Foundation Endowment Fund. G.D.Z.W. was supported by the Chateaubriand Fellowship of the Office for Science & Technology of the Embassy of France in the United States and by the Duke University Graduate Student International Dissertation Research Travel Fellowship. The authors would also like to thank R. Grigoryan (Duke) and G.S. Dwyer (Duke) for aid with analytical methods and R.C. Hill (Duke), M. Petrović (Ruđer Bošković Institute), G.A. Hall (Duke), and H. Wudke (Duke) for support with sample collection and lab activities. This work was performed in part at the Duke University Shared Materials Instrumentation Facility (SMIF), a member of the North Carolina Research Triangle Nanotechnology Network (RTNN), which is supported by the National Science Foundation (ECCS-2025064) as part of the National Nanotechnology Coordinated Infrastructure (NNCI). We thank two anonymous reviewers and the Editor Dr. Horner for their thorough and detailed reviews, which have improved the quality of this paper.

Supplementary materials

Supplementary material associated with this article can be found, in the online version, at doi:10.1016/j.epsl.2026.119849.

Data availability

All data are provided in Supplement

References

Alonso, R.N., 1999. On the origin of La Puna Borates. Acta Geol. Hisp. 141–166.

Alonso, R.N., Viramonte, J.G., 1990. Borate deposits in the Andes. In: Fontboté, L., Amstutz, G.C., Cardozo, M., Cedillo, E., Frutos, J. (Eds.), Stratabound Ore Deposits in the Andes. Springer, Berlin, Heidelberg, pp. 721–732. https://doi.org/10.1007/978-3-642-88282-1_57.

Álvarez-Amado, F., Tardani, D., Poblete-González, C., Godfrey, L., Matte-Estrada, D., 2022. Hydrogeochemical processes controlling the water composition in a hyperarid environment: new insights from Li, B, and Sr isotopes in the Salar de Atacama. Sci. Total Environ. 835, 155470. https://doi.org/10.1016/j.scitotenv.2022.155470.

Baker, P.A., Rigsby, C.A., Seltzer, G.O., Fritz, S.C., Lowenstein, T.K., Bacher, N.P., Veliz, C., 2001. Tropical climate changes at millennial and orbital timescales on the Bolivian Altiplano. Nature 409, 698–701. https://doi.org/10.1038/35055524.

Bobst, A.L., Lowenstein, T.K., Jordan, T.E., Godfrey, L.V., Ku, T.-L., Luo, S., 2001. A 106 ka paleoclimate record from drill core of the Salar de Atacama, northern Chile. Palaeogeogr. Palaeoclimatol. Palaeoecol. 173, 21–42. https://doi.org/10.1016/S0031-0182(01)00308-X.

Borda, L.G., Godfrey, L.V., Del Bono, D.A., Blanco, C., García, M.G., 2023. Low-temperature geochemistry of B in a hypersaline basin of Central Andes: insights from mineralogy and isotopic analysis ($\delta^{11}B$ and $^{87}Sr/^{86}Sr$). Chem. Geol. 635, 121620. https://doi.org/10.1016/j.chemgeo.2023.121620.

Boschetti, T., Cortecci, G., Barbieri, M., Mussi, M., 2007. New and past geochemical data on fresh to brine waters of the Salar de Atacama and Andean Altiplano, northern Chile. Geofluids 7, 33–50. https://doi.org/10.1111/j.1468-8123.2006.00159.x.
CAMIBOL, 2016. Gerencia Nacional de Recursos Evaporíticos Memoria 2016. Corporación Minera de Bolivia.
Chong, G., Pueyo, J.J., Demergasso, C., 2000. Los yacimientos de boratos de Chile. Rev. Geol. Chile 27, 99–119.
Cortes-Calderon, E.A., Ellis, B.S., Tavazzani, L., Magna, T., Harris, C., Benson, T.R., 2025. Lithium Inventory of the Cerro Galán Volcanic System (Argentina): the role of magmatism as a source for Li-bearing brine deposits. Econ. Geol. https://doi.org/10.5382/econgeo.5154.
Ericksen, G.E., Salas, R., 1987. Geology and Resources of the Salars in the Central Andes (Open-File Report No. 88–210), Open-File Report. U.S. Geological Survey.
Ericksen, G.E., Vine, J.D., Raul Ballón, A., 1978. Chemical composition and distribution of lithium-rich brines in salar de Uyuni and nearby salars in southwestern Bolivia. Energy 3, 355–363. https://doi.org/10.1016/0360-5442(78)90032-4.
Eugster, H.P., Hardie, L.A., 1978. Saline Lakes. In: Lerman, A. (Ed.), Lakes: Chemistry, Geology, Physics. Springer, New York, NY, pp. 237–293. https://doi.org/10.1007/978-1-4757-1152-3_8.
Eugster, H.P., Jones, B.F., 1979. Behavior of major solutes during closed-basin brine evolution. Am. J. Sci. 279, 609–631. https://doi.org/10.2475/ajs.279.6.609.
Fornari, M., Risacher, F., Féraud, G., 2001. Dating of paleolakes in the central Altiplano of Bolivia. Palaeogeogr. Palaeoclimatol. Palaeoecol. 172, 269–282. https://doi.org/10.1016/S0031-0182(01)00301-7.
Fritz, S.C., Baker, P.A., Lowenstein, T.K., Seltzer, G.O., Rigsby, C.A., Dwyer, G.S., Tapia, P.M., Arnold, K.K., Ku, T.-L., Luo, S., 2004. Hydrologic variation during the last 170,000 years in the southern hemisphere tropics of South America. Quat. Res. 61, 95–104. https://doi.org/10.1016/j.yqres.2003.08.007.
Garcia, M.G., Borda, L.G., Godfrey, L.V., López Steinmetz, R.L., Losada-Calderon, A., 2020. Characterization of lithium cycling in the Salar De Olaroz, Central Andes, using a geochemical and isotopic approach. Chem. Geol. 531, 119340. https://doi.org/10.1016/j.chemgeo.2019.119340.
Garrett, D.E., 2004. Part 1 - lithium. In: Garrett, D.E. (Ed.), Handbook of Lithium and Natural Calcium Chloride. Academic Press, Oxford, pp. 1–235. https://doi.org/10.1016/B978-012276152-2/50037-2.
Godfrey, L., Álvarez-Amado, F., 2020. Volcanic and saline lithium inputs to the Salar de Atacama. Minerals 10, 201. https://doi.org/10.3390/min10020201.
Godfrey, L.V., Chan, L.-H., Alonso, R.N., Lowenstein, T.K., McDonough, W.F., Houston, J., Li, J., Bobst, A., Jordan, T.E., 2013. The role of climate in the accumulation of lithium-rich brine in the Central Andes. Appl. Geochem. 38, 92–102. https://doi.org/10.1016/j.apgeochem.2013.09.002.
Grove, M.J., Baker, P.A., Cross, S.L., Rigsby, C.A., Seltzer, G.O., 2003. Application of strontium isotopes to understanding the hydrology and paleohydrology of the Altiplano, Bolivia–Peru. Palaeogeogr. Palaeoclimatol. Palaeoecol. Late-quat. Palaeoclim. South. Trop. Andes Adjac. Reg. 194, 281–297. https://doi.org/10.1016/S0031-0182(03)00282-7.
Gruber, P.W., Medina, P.A., Keoleian, G.A., Kesler, S.E., Everson, M.P., Wallington, T.J., 2011. Global lithium availability. J. Ind. Ecol. 15, 760–775. https://doi.org/10.1111/j.1530-9290.2011.00359.x.
Haferburg, G., Gröning, J.A.D., Schmidt, N., Kummer, N.-A., Erquicia, J.C., Schlömann, M., 2017. Microbial diversity of the hypersaline and lithium-rich Salar de Uyuni, Bolivia. Microbiol. Res. 199, 19–28. https://doi.org/10.1016/j.micres.2017.02.007.
Hall, G.A., Williams, G.D.Z., Sirbescu, M.-L.C., Lu, P.L., Dwyer, G.S., Richter, D.D., Vengosh, A., 2025. Strontium isotopes and Rb/Sr tracers in surface soils for locating subsurface lithium pegmatites. Appl. Geochem. 195, 106631. https://doi.org/10.1016/j.apgeochem.2025.106631.
Hardie, L.A., Eugster, H.P., 1970. The evolution of closed-basin brines. Mineral. Soc. Am. Spec. Pap. 3, 273–290.
IEA, 2021. The Role of Critical Minerals in Clean Energy Transitions. International Energy Agency, Paris.
Jaskula, B.W., 2024. Lithium, Mineral Commodity Summaries 2024. U.S. Geological Survey.
Jochum, K.P., Nohl, U., Herwig, K., Lammel, E., Stoll, B., Hofmann, A.W., 2005. GeoReM: A new geochemical database for reference materials and isotopic standards. Geostand. Geoanalytical Res. 29, 333–338. https://doi.org/10.1111/j.1751-908X.2005.tb00904.x.
Kasemann, S.A., Meixner, A., Erzinger, J., Viramonte, J.G., Alonso, R.N., Franz, G., 2004. Boron isotope composition of geothermal fluids and borate minerals from salar deposits (central Andes/NW Argentina). J. S. Am. Earth Sci. 16, 685–697. https://doi.org/10.1016/j.jsames.2003.12.004.
López Steinmetz, R.L., Salvi, S., Gabriela García, M., Peralta Arnold, Y., Béziat, D., Franco, G., Constantini, O., Córdoba, F.E., Caffe, P.J., 2018. Northern Puna Plateau-scale survey of Li brine-type deposits in the Andes of NW Argentina. J. Geochem. Explor. 190, 26–38. https://doi.org/10.1016/j.gexplo.2018.02.013.
López Steinmetz, R.L., Salvi, S., Sarchi, C., Santamans, C., López Steinmetz, L.C., 2020. Lithium and brine geochemistry in the salars of the southern Puna, Andean Plateau of Argentina. Econ. Geol. 115, 1079–1096. https://doi.org/10.5382/econgeo.4754.
Lowenstein, T.K., Risacher, F., 2009. Closed Basin brine evolution and the influence of Ca–Cl inflow waters: Death Valley and Bristol Dry Lake California, Qaidam Basin, China, and Salar de Atacama, Chile. Aquat. Geochem. 15, 71–94. https://doi.org/10.1007/s10498-008-9046-z.
Marazuela, M.A., Vázquez-Suñé, E., Ayora, C., García-Gil, A., Palma, T., 2019. The effect of brine pumping on the natural hydrodynamics of the Salar de Atacama: The damping capacity of salt flats. Sci. Total Environ. 654, 1118–1131. https://doi.org/10.1016/j.scitotenv.2018.11.196.
McCaffrey, M.A., Lazar, B., Holland, H.D., 1987. The evaporation path of seawater and the coprecipitation of Br- and K+ with halite. J. Sediment. Res. 57, 928–937. https://doi.org/10.1306/212F8CAB-2B24-11D7-8648000102C1865D.
Meixner, A., Alonso, R.N., Lucassen, F., Korte, L., Kasemann, S.A., 2022. Lithium and Sr isotopic composition of salar deposits in the Central Andes across space and time: the Salar de Pozuelos, Argentina. Min. Depos. 57, 255–278. https://doi.org/10.1007/s00126-021-01062-3.
Mihalasky, M.J., Briggs, D.A., Baker, M., Jaskula, B., Cheriyan, K., Deloach-Overton, S. W., 2020. Lithium occurences and processing facilities of Argentina, and salars of the Lithium Triangle, Central South America. https://doi.org/10.5066/P9RLUH4F.
Millot, R., Guerrot, C., Vigier, N., 2004. Accurate and high-precision measurement of lithium isotopes in two reference materials by MC-ICP-MS. Geostand. Geoanalytical Res. 28, 153–159. https://doi.org/10.1111/j.1751-908X.2004.tb01052.x.
Moon, J.W., 2024. The mineral industry of China. 2020-2021 Minerals Yearbook 9.1-9.46.
Moraga, A., Chong, G., Fortt, M.A., Henriquez, H., 1974. Estudio Geologico del Salar de Atacama, Provincia de Antofagasta (Boletin). Instituto de Investigaciones Geologicas.
Muller, E., Gaucher, E.C., Durlet, C., Moquet, J.S., Moreira, M., Rouchon, V., Louvat, P., Bardoux, G., Noirez, S., Bougeault, C., Vennin, E., Gérard, E., Chavez, M., Virgone, A., Ader, M., 2020. The origin of continental carbonates in Andean salars: A multi-tracer geochemical approach in Laguna Pastos Grandes (Bolivia). Geochim. Cosmochim. Acta 279, 220–237. https://doi.org/10.1016/j.gca.2020.03.020.
Munk, L.A., Boutt, D., Butler, K., Russo, A., Jenckes, J., Moran, B., Kirshen, A., 2025. Lithium brines: origin, characteristics, and global distribution. Econ. Geol. 120, 575–597. https://doi.org/10.5382/econgeo.5134.
Munk, L.A., Boutt, D.F., Hynek, S.A., Moran, B.J., 2018. Hydrogeochemical fluxes and processes contributing to the formation of lithium-enriched brines in a hyper-arid continental basin. Chem. Geol. 493, 37–57. https://doi.org/10.1016/j.chemgeo.2018.05.013.
Nunnery, J.A., 2012. Ph.D. Duke University, Durham, NC.
Nunnery, J.A., Fritz, S.C., Baker, P.A., Salenbien, W., 2019. Lake-level variability in Salar de Coipasa, Bolivia during the past ~40,000 yr. Quat. Res. 91, 881–891. https://doi.org/10.1017/qua.2018.108.
Oi, T., Nomura, M., Musashi, M., Ossaka, T., Okamoto, M., Kakihana, H., 1989. Boron isotopic compositions of some boron minerals. Geochim. Cosmochim. Acta 53, 3189–3195. https://doi.org/10.1016/0016-7037(89)90099-9.
Orberger, B., Rojas, W., Millot, R., Flehoc, C., 2015. Stable isotopes (Li, O, H) combined with brine chemistry: powerful tracers for Li origins in Salar deposits from the Puna Region, Argentina. In: Procedia Earth and Planetary Science, 11th Applied Isotope Geochemistery Conference AIG-11, 13, pp. 307–311. https://doi.org/10.1016/j.proeps.2015.07.072.
Orris, G.J., 1995. Borate Deposits (Open-File Report No. 95–842). U.S. Geological Survey.
Palmer, M.R., Helvaci, C., 1995. The boron isotope geochemistry of the Kirka borate deposit, western Turkey. Geochim. Cosmochim. Acta 59, 3599–3605. https://doi.org/10.1016/0016-7037(95)00227-Q.
Parkhurst, D.L., Appelo, C.A.J., 2013. Description of input and examples for PHREEQC version 3: a computer program for speciation, batch-reaction, one-dimensional transport, and inverse geochemical calculations (No. 6-A43). Description of Input and Examples for PHREEQC Version 3: A Computer Program for Speciation, Batch-Reaction, One-Dimensional Transport, and Inverse Geochemical Calculations. Techniques and Methods. U.S. Geological Survey, Reston, VA. https://doi.org/10.3133/tm6A43.
Penniston-Dorland, S., Liu, X.-M., Rudnick, R.L., 2017. Lithium isotope geochemistry. Rev. Mineral. Geochem. 82, 165–217. https://doi.org/10.2138/rmg.2017.82.6.
Placzek, C., Quade, J., Patchett, P.J., 2006. Geochronology and stratigraphy of late pleistocene lake cycles on the southern Bolivian Altiplano: implications for causes of tropical climate change. GSA Bull. 118, 515–532. https://doi.org/10.1130/B25770.1.
Placzek, C.J., Quade, J., Patchett, P.J., 2013. A 130 ka reconstruction of rainfall on the Bolivian Altiplano. Earth Planet. Sci. Lett. 363, 97–108. https://doi.org/10.1016/j.epsl.2012.12.017.
Placzek, C.J., Quade, J., Patchett, P.J., 2011. Isotopic tracers of paleohydrologic change in large lakes of the Bolivian Altiplano. Quat. Res. 75, 231–244. https://doi.org/10.1016/j.yqres.2010.08.004.
Pueyo, J.J., Chong, G., Ayora, C., 2017. Lithium saltworks of the Salar de Atacama: a model for $MgSO_4$-free ancient potash deposits. Chem. Geol. 466, 173–186. https://doi.org/10.1016/j.chemgeo.2017.06.005.
Rettig, S.L., Jones, B.F., Risacher, F., 1980. Geochemical evolution of brines in the Salar of Uyuni, Bolivia. Chem. Geol. 57–79. https://doi.org/10.1016/0009-2541(80)90116-3.
Risacher, F., 1992. Géochimie des lacs salés et croûtes de sel de l'altiplano bolivien. Sgeol 45, 135–214. https://doi.org/10.3406/sgeol.1992.1889.
Risacher, F., Alonso, H., Salazar, C., 2003. The origin of brines and salts in Chilean salars: a hydrochemical review. Earth-Sci. Rev. 63, 249–293. https://doi.org/10.1016/S0012-8252(03)00037-0.
Risacher, F., Alonso, H., Salazar, C., 1999. Geoquímica en Cuencas Cerradas: I, II y III (No. 51). Convenio de Cooperación DGA-UCN-Orstom, Santiago.
Risacher, F., Fritz, B., 2009. Origin of salts and brine evolution of Bolivian and Chilean salars. Aquat Geochem 15, 123–157. https://doi.org/10.1007/s10498-008-9056-x.
Risacher, F., Fritz, B., 2000. Bromine geochemistry of salar de uyuni and deeper salt crusts, Central Altiplano, Bolivia. Chem. Geol. 167, 373–392. https://doi.org/10.1016/S0009-2541(99)00251-X.

Risacher, F., Fritz, B., 1992. Mise en évidence d'une phase climatique holocène extrêmement aride dans l'Altiplano central, par la présence de la polyhalite dans le salar de Uyuni (Bolivie). C. R. Acad. Sci. Paris 2 (314), 1371–1377.
Risacher, F., Fritz, B., 1991a. Geochemistry of Bolivian salars, Lipez, southern Altiplano: origin of solutes and brine evolution. Geochim. Cosmochim. Acta 55, 687–705. https://doi.org/10.1016/0016-7037(91)90334-2.
Risacher, F., Fritz, B., 1991b. Quaternary geochemical evolution of the salars of Uyuni and Coipasa, Central Altiplano, Bolivia. Chem. Geol. 211–231. https://doi.org/10.1016/0009-2541(91)90101-V.
Risacher, F., Fritz, B., Hauser, A., 2011. Origin of components in Chilean thermal waters. J. S. Am. Earth Sci. 31, 153–170. https://doi.org/10.1016/j.jsames.2010.07.002.
Sarchi, C., Lucassen, F., Meixner, A., Caffe, P.J., Becchio, R., Kasemann, S.A., 2023. Lithium enrichment in the Salar de Diablillos, Argentina, and the influence of cenozoic volcanism in a basin dominated by paleozoic basement. Min. Depos. 58, 1351–1370. https://doi.org/10.1007/s00126-023-01181-z.
Schmidt, N., 2010. Hydrogeological and hydrochemical investigations at the Salar de Uyuni (Bolivia) with regard to the extraction of lithium. Freib. Online Geol. 26, 101.
Servant, M., Fontes, J.C., 1978. Les lacs quaternaires des hauts plateaux des Andes boliviennes : premières interprétations paléoclimatiques. Cah. ORSTOM Sér. Géol. 10, 9–23.
Sieland, R., 2014. Hydraulic investigations of the Salar de Uyuni, Bolivia. Freib. Online Geol. 37, 208.
Sieland, R., Schmidt, N., Schön, A., Schreckenbach, J., Merkel, B., 2011. Geochemische, Hydrogeologische und Feinstratigraphische Untersuchungen am Salar de Uyuni (Bolivien). TU Bergakademie Freiberg, Freiberg.
Vila, T., 1990. Salar deposits in Northern Chile. In: Fontboté, L., Amstutz, G.C., Cardozo, M., Cedillo, E., Frutos, J. (Eds.), Stratabound Ore Deposits in the Andes. Springer, Berlin, Heidelberg, pp. 703–720. https://doi.org/10.1007/978-3-642-88282-1_56.
Williams, G.D.Z., Nativ, P., Vengosh, A., 2025a. The role of boron in controlling the pH of lithium brines. Sci. Adv. 11, eadw3268. https://doi.org/10.1126/sciadv.adw3268.
Williams, G.D.Z., Petrović, M., Hill, R.C., Hall, G.A., Vengosh, A., 2025b. The water quality impacts of legacy hard-rock lithium mining and processing. Environ. Sci. Technol. 59, 16492–26505. https://doi.org/10.1021/acs.est.5c13682.
Williams, G.D.Z., Saltman, S., Wang, Z., Warren, D.M., Hill, R.C., Vengosh, A., 2024. The potential water quality impacts of hard-rock lithium mining: insights from a legacy pegmatite mine in North Carolina, USA. Sci. Total Environ. 956, 177281. https://doi.org/10.1016/j.scitotenv.2024.177281.
Williams, G.D.Z., Vengosh, A., 2025. Quality of wastewater from lithium-brine mining. Environ. Sci. Technol. Lett. 12, 151–157. https://doi.org/10.1021/acs.estlett.4c01124.
YLB, 2019. Memoria Institucional 2019. Yacimientos de Litio Bolivianos.
Zheng, M., Liu, X., 2009. Hydrochemistry of salt lakes of the Qinghai-Tibet Plateau, China. Aquat. Geochem. 15, 293–320. https://doi.org/10.1007/s10498-008-9055-y.
Zherebtsova, I.K., Volkova, N.N., 1966. Experimental study of behavior of trace elements in the process of natural solar evaporation of Black Sea water and Sasyk-Sivash brine. Geochem. Int. 3, 656–670.